Molecular Motions in Metal-Containing Polymers: Solid-State Deuterium NMR Studies of Polyferrocenylsilanes near Their Glass Transition Temperature

Kevin Kulbaba,[†] Ian Manners,*[,†] and Peter M. Macdonald*[,†,‡]

Department of Chemistry, University of Toronto, 80 St. George Street, Toronto, Ontario, Canada M5S 3H6, and Department of Chemistry, University of Toronto at Mississauga, 3359 Mississauga Road, Mississauga, Ontario, Canada L5L 1C6

Received July 16, 2002; Revised Manuscript Received October 2, 2002

ABSTRACT: The molecular motions in polyferrocenylsilanes, a novel class of metal-containing polymers with a main chain of alternating ferrocene and organosilane units, have been probed using variable temperature solid-state ^{2}H NMR. Polyferrocenylsilanes with selective deuteration of either the cyclopentadienyl ligands of the ferrocene units or the side groups attached to silicon were prepared by ring-opening polymerization methodologies. The polymer backbone motions in the ferrocene-deuterated materials, poly(ferrocenyl-d_8-dimethylsilane) [Fe(η-C_5D_4)$_2$Si(CH_3)$_2$]$_n$ (**2a**, T_g = 33 °C), poly(ferrocenyl-d_8-dimethoxysilane) [Fe(η-C_5D_4)$_2$Si(OCH_3)$_2$]$_n$ (**2b**, T_g = 19 °C), and poly(ferrocenyl-d_8-dihexyloxysilane) [Fe(η-C_5D_4)$_2$Si(OC_6H_{13})$_2$]$_n$ (**2c**, T_g = −51 °C) were examined over a temperature range of −50 to +125 °C. The ^{2}H NMR spectra of all three polymers indicated that the cyclopentadienyl groups were static at temperatures below the particular mechanical T_g. At temperatures just above T_g the cyclopentadienyl rings began to undergo slow small-angle oscillations. These motions increased in both rate and angle of excursion until, at a temperature approximately 50−70 °C above the particular mechanical T_g, the polymers underwent a transition to a regime characterized by rapid isotropic motional averaging. The silicon side group motions were also examined over the same temperature range using the corresponding poly(ferrocenyldimethyl-d_3-silane) [Fe(η-C_5H_4)$_2$Si(CH_3)(CD_3)]$_n$ (**2d**, T_g = 33 °C) and poly(ferrocenyldimethoxy-d_6-silane) [Fe(η-C_5H_4)$_2$Si(OCD_3)$_2$]$_n$ (**2e**, T_g = 19 °C). For polymer **2d** the ^{2}H NMR spectra showed the presence of fast methyl rotation about the Si−CD_3 bond even at temperatures below the mechanical T_g. For polymer **2e**, the ^{2}H NMR spectra showed the presence of fast methyl rotations about the O−CD_3 bond combined with a discrete jumping motion about the Si−O bond. Increasing temperature brought about spectral changes reflecting a superposition of backbone and side-chain motions. At temperatures 50−70 °C above the respective mechanical T_g the ^{2}H NMR spectra of both **2d** and **2e** were isotropically narrowed, reflecting the onset of isotropic motions of the polymer backbone.

Introduction

The physical properties of a polymeric material depend on the structure, order, and dynamics of the macromolecular chains.[1] Furthermore, properties such as the conductivity and electronic transitions of macromolecules may depend on the molecular conformations present in the solid state. Understanding the motions of polymer chains in a bulk material therefore represents an important scientific challenge and has implications for the observed mechanical properties and possible applications of the polymer. To date, however, virtually all studies in this area have focused on organic polymers.[2,3]

The incorporation of transition metal centers with unusual coordination geometry in the polymer main chain is of considerable interest as this should lead to an increase in the range of motions possible in comparison to organic polymer systems.[4] High molecular weight ($M_w = 10^5-10^6$, $M_n > 10^5$) polyferrocenylsilanes (PFSs) **2** represent a recently established class of organometallic materials with a main chain consisting of ferrocene and organosilane units.[5] These novel, well-characterized, metal-containing polymers are readily accessible via the ring-opening polymerization (ROP) of strained metallocenophane monomers such as **1**.[5,6] Recent work on PFSs has focused on their interesting conformational and morphological properties[7−10] and on their applications as redox-active gels,[11] variable refractive index sensors,[12] electron beam resistant and charge dissipative coatings,[13] and precursors to ceramics with tunable magnetic properties over a range of length scales.[14−16] Water-soluble PFSs have been prepared recently and are of interest for layer-by-layer self-assembly applications.[17−20] In addition, PFS block copolymers with inorganic[21] and organic coblocks[22] have been developed by our group using a living anionic or transition-metal-catalyzed ROP approach.[21−23] These materials generate self-assembled nanoscale structures in solution and in the solid state and are of interest as etch resists and as precursors to ceramic patterns on the nanometer scale.[24−28]

The physical properties of PFSs are found to be highly dependent on the substituents at silicon. For instance, symmetrically substituted PFSs with relatively small substituents (e.g., R = methyl, *n*-propyl, *n*-butyl, *n*-pentyl) are semicrystalline, while substitution with unsymmetrical or larger alkyl groups (e.g., R = *n*-hexyl) at silicon affords amorphous polymers. The mechanical glass transition temperature (T_g) is also affected sig-

[†] University of Toronto.
[‡] University of Toronto at Mississauga.
* To whom correspondence should be addressed. I. Manners: Tel 416 978 6157; Fax 416 978 6157; e-mail imanners@chem.utoronto.ca. P. M. Macdonald: Tel 905 828 3805; Fax 905 828 5425; e-mail pmacdona@utm.utoronto.ca.

10.1021/ma021130q CCC: $22.00
Published on Web 12/02/2002

nificantly by the substituents at silicon with values ranging from as low as −72 °C for poly(ethylene glycol) methyl ether substituted PFSs[28] to +90 °C for poly(ferrocenylmethylphenylsilane).[6]

Substantial changes in the mechanical properties of polymers are observed near T_g, and these are certainly directly related to molecular motions of the polymer main chain and side groups. Although the vast majority of studies in this area have focused on organic materials, a few studies of motions in ferrocene-containing polymers using Mössbauer spectroscopy have been reported in the literature, particularly by Nuyken and co-workers.[29] The backbone motions in particular are potentially unusual in polyferrocenes, since ferrocene itself possesses a rather facile (almost free) cyclopentadienyl (Cp) ligand rotation.[30] How such motions are constrained by inclusion of ferrocene within a polymer main chain, and by the preference of the Cp ligands of ferrocene to remain approximately coplanar with one another, are intriguing questions.

Solid-state ^{2}H NMR spectroscopy is uniquely suited to the study of molecular motions of organic polymers, including the effects of temperature relative to the glass transition.[31] Deuteron labels are nonperturbing and, provided suitable synthetic pathways are available, may be placed at any desired location within a polymer chain. The ^{2}H NMR spectral line shape sensitively reflects details of the nature and rates of any molecular motions present. As well, the spin−lattice relaxation time (T_1) is dominated by quadrupolar relaxation mechanisms and, therefore, reflects a single effective correlation time for molecular motions.[32]

In this paper we report ^{2}H NMR studies of several high molecular weight PFSs, having different side groups at silicon and, therefore, different mechanical T_g's.[6,33] The first is poly(ferrocenyldimethylsilane) (**2a,d**, R = Me), the most intensively studied PFS and the prototypical example of these materials. Poly(ferrocenyldimethylsilane) is semicrystalline with a T_g of 33 °C and a T_m in the 122−145 °C range, where the exact value of the latter depends on sample thermal history.[6,9,10] X-ray structural studies of well-defined oligoferrocenyldimethylsilanes such as the linear pentamer show a parallel packing of trans planar zigzag polymer chains, and an analogous packing is suggested to occur in the high polymer as the X-ray diffraction patterns are very similar.[7,10] More recently, detailed X-ray work by Papkov and Pannell on polyferrocenyldimethylsilanes has revealed the coexistence of 3D monoclinic crystalline polymer phases and a 2D mesophase with hexagonal or tetragonal packing of the macromolecules.[9] The authors suggest that the coexistence of these phases is most likely a result of the close energies of the various conformations of the polymer backbone. This explanation is in line with the results of conformational calculations by O'Hare and co-workers.[8] It is of interest to examine whether differences in molecular motions exist between these various phases.

The second is poly(ferrocenyldimethoxysilane) (**2b,e**, R = OMe). The initial samples of this material studied by our group were amorphous with a T_g of 19 °C.[34] Recently, we have found that the material will crystallize upon thermal annealing, and a T_m was detected in the range of 80−103 °C by DSC depending on the thermal history of the sample.[35]

The third is poly(ferrocenyldihexyloxysilane) (**2c,** R = OC_6H_{13}), an amorphous polymer with a mechanical T_g of −51 °C. Such a low-T_g polymeric material was expected to provide an excellent opportunity to study molecular motions in a highly mobile PFS main chain.

^{2}H NMR spectra were obtained for these three different PFSs over a range of temperatures (−50 to 125 °C) spanning the respective mechanical T_g's. The polymers were deuterio-labeled at either the Cp rings (**2a**−**c**) or the side groups at silicon (**2d,e**). For each polymer at each temperature, the ^{2}H NMR line shape was analyzed to extract the nature and the rate of motion present using the method of Vold and co-workers.[36]

Experimental Section

Equipment and Materials. All reactions and manipulations were carried out under an atmosphere of prepurified nitrogen using either Schlenk techniques or an inert-atmosphere glovebox (Innovative Technologies), and all solvents were dried by standard methods unless otherwise stated. The solution 400 MHz ^{1}H, 100 MHz ^{13}C, and 79 MHz ^{29}Si NMR for compounds **2a**−**e** were recorded on a Varian Unity 400 spectrometer. A Perkin-Elmer DSC-7 differential scanning calorimeter equipped with a TAC 7 instrument controller was used to study the thermal behavior of poly(ferrocenyldimethoxysilane). The thermograms were calibrated with the melting transitions of decane and indium and were obtained at a heating rate of 10 °C/min from 0 to 180 °C.

Molecular weights were determined by gel permeation chromatography (GPC) using a Waters Associates 2690 separation module that has as components an inline solvent degaser, a HPLC pump, and an autosampler. The separation module was equipped with a Waters 410 differential refractometer detector as the concentration detector. Columns from Polymer Laboratories with pore sizes of 5×10^2, 1×10^3, and 1×10^5 Å were used with the eluent THF at a flow rate of 1.0 mL min^{-1}. Polystyrene standards purchased from Aldrich were used for calibration.

Synthesis of 2a. To increase the degree of deuterium substitution on the Cp rings (in excess of 90% substitution), a modification of the methods developed by Hamon and co-workers[37] was used. To a solution of 50 mL of DMSO and 50 mL of freshly distilled Cp (372 mmol), 50 mL of a 20 mol % mixture of NaOD in D_2O was added, and the reaction mixture was stirred vigorously for 1 h at 2 °C. The aqueous phase was decanted off, and a fresh 50 mL of NaOD/D_2O was added and the reaction stirred for a further hour. This process was repeated three more times for a total of five aliquots of the NaOD solution. The deuterated product, Cp-d_6, was isolated by decantation and purified by distillation under an atmosphere of prepurified N_2 affording 37 mL (275 mmol, 74% yield). The deuterated ferrocene was synthesized by literature procedures[45] using 35 mL of freshly distilled Cp-d_6 (260 mmol), 21.9 g (172 mmol) of iron dichloride, and 4.1 g (73 mmol) of iron filings. The orange solid was extracted using dichloromethane and water, recrystallized from hexanes, and further purified by vacuum sublimation to give 14.3 g (43% yield) with approximately 95% deuteration of the Cp−H sites by mass spectrometry. The monomer was synthesized and then polymerized using transition-metal-catalyzed ring-opening polymerization with a Pt(0) catalyst (Karstedt's catalyst) by previously reported techniques.[5,6] The purity was assessed using ^{1}H NMR and determined to be sufficient for this study. Monomer **1a**: red crystals; yield 79%. ^{1}H NMR (C_6D_6, 400 MHz): δ 4.40 (m, 0.3 H, Cp), 3.94 (m, 0.3 H, Cp), 0.36 (s, 6 H, CH_3) ppm. Polymer **2a**: amber fibrous solid; yield 69%. ^{1}H NMR (C_6D_6, 400 MHz): δ 4.27 (m, 0.3 H, Cp) 4.11 (m, 0.3 H, Cp), 0.55 (s, 6 H, CH_3) ppm. GPC (THF vs polystyrene standards): 512 000 (M_w), 2.2 (PDI). The degree of deuteration of the polymer was estimated to be ca. 92% by ^{1}H NMR integration.

Synthesis of 2b. Deuteration of the Cp rings of ferrocene was achieved by analogous methods to the case of **2a**. The monomer was prepared by previously reported methods and polymerized using transition-metal-catalyzed ring-opening

polymerization with a Pt(0) catalyst (Karstedt's catalyst).[6,34] Monomer **1b:** red crystals; yield 75%. ^{1}H NMR (C_6D_6, 400 MHz): δ 4.40 (m, 0.2 H, Cp), 4.13 (m, 0.2 H, Cp) 3.62 (s, 6 H, CH_3) ppm. Polymer **2b**: amber gum; yield 66%. ^{1}H NMR (C_6D_6, 400 MHz): δ 4.54 (m, 0.2 H, Cp), 4.44 (m, 0.2 H, Cp), 3.65 (s, 6 H, CH_3) ppm. GPC: 422 000 (M_w), 2.9 (PDI). The degree of deuteration of the polymer was estimated to be ca. 95% by ^{1}H NMR.

Synthesis of 2c. Deuteration of the Cp rings of ferrocene was achieved by analogous methods to the case of **2a**. The monomer was prepared by previously reported methods and polymerized using transition-metal-catalyzed ring-opening polymerization with a Pt(0) catalyst (Karstedt's catalyst).[4,34] Monomer **1c**: red liquid; yield 75%. ^{1}H NMR (C_6D_6, 400 MHz): δ 4.44 (m, 0.2 H, Cp), 4.22 (m, 0.2 H, Cp), 4.08 (t, 4 H, CH_2), 1.71 (m, 4 H, CH_2), 1.42 (m, 4 H, CH_2), 1.27 (m, 8 H, CH_2), 0.89 (t, 6 H, CH_3). Polymer **2c**: red gum; yield (0.75 g, 83%). ^{1}H NMR (C_6D_6, 400 MHz): δ 4.68 (m, 0.2 H, Cp), 4.52 (m, 0.2 H, Cp), 4.05 (t, 4 H, CH_2), 1.72 (m, 4 H, CH_2), 1.53 (m, 4 H, CH_2), 1.36 (m, 8 H, CH_2), 0.96 ppm (t, 6 H, CH_3). GPC: 158 000 (M_w), 2.2 (PDI). The degree of deuteration of the polymer was estimated to be ca. 94% by ^{1}H NMR integration.

Synthesis of 2d. Polymer **2d** was synthesized via direct halide substitution of poly(ferrocenylchloromethylsilane) with Me-d_3 Li in THF using methods analogous to those reported previously.[38] Analysis of the ^{1}H NMR of the product showed that essentially all of the chlorine substituents on the polymer were replaced with CD_3 groups. Polymer **2d**: amber fibrous solid; yield 74%. ^{1}H NMR (C_6D_6, 400 MHz): δ 4.27 (m, 4 H, Cp), 4.10 (m, 4 H, Cp), 0.55 ppm (s, 3 H, CH_3). GPC: 22 000 (M_w), 1.9 (PDI). Powder X-ray diffraction studies showed the material to be moderately crystalline with an approximate degree of crystallinity of 50%, similar to that observed previously.[6,9] Deuteration was confirmed to be ca. 50% by ^{1}H NMR integration.

Synthesis of 2e. Synthesis of **2e** was carried out by the reaction of 2 equiv of methanol-d_4 with the $SiCl_2$-bridged monomer followed by ROP via a procedure analogous to that recently reported for the nondeuterated counterpart.[34] Monomer **1e**: red crystals; yield 87%. ^{1}H NMR (C_6D_6, 400 MHz): δ 4.40 (m, 4 H, Cp), 4.13 (m, 4 H, Cp) ppm. Polymer **2e**: amber fibers; yield 69%. ^{1}H NMR (C_6D_6, 400 MHz): δ 4.54 (m, 4 H, Cp), 4.43 ppm (m, 4 H, Cp). GPC: 606 000 (M_w), 1.9 (PDI). Powder X-ray diffraction studies showed the material to be semicrystalline after thermal annealing at 60 °C for 48 h under vacuum.[35]

Solid-State ^{2}H NMR Spectroscopy. Variable temperature ^{2}H NMR spectra of the deuterated polymers **2a,b,d,e** were obtained on a Varian Unity 200 MHz spectrometer operating at 30.72 MHz for deuterium. The quadrupolar echo pulse sequence was employed using a spectral width of 1 MHz, a 90 pulse width of 2.5 μs, and an interpulse delay of 55 μs for **2a,b**. For **2d,e** a spectral width of 500 kHz was employed, with a 90° pulse width of 2.0 μs and an interpulse delay of 55 μs. Spectra for polymer **2c** were obtained on a Chemagnetics CMX300 NMR spectrometer operating at 45.98 MHz for deuterium, using a Chemagnetics static solids probe. The quadrupolar echo pulse sequence was employed with a spectral width of 1 MHz, a 90° pulse width of 2 μs, and an interpulse delay of 30 μs. In all cases the recycle delay was equivalent to at least 5T_1. Typically, 1000 FIDs were signal averaged, digitized into 1K data points, and Fourier transformed after being subjected to exponential multiplication equivalent to line broadening of 1000 Hz. Temperature was controlled by passing liquid nitrogen boil-off gas through a heater before being routed to the sample within the NMR probe. The heater was controlled by a feedback loop to a temperature sensing thermocouple at the sample. The samples were equilibrated a minimum of 30 min at a given temperature prior to beginning signal acquisition. For T_1 relaxation time measurements an inversion−recovery sequence was combined with the quadrupolar echo pulse sequence, and the T_1 was obtained in the usual fashion from the dependence of the spectral intensity on the recovery time.

Scheme 1

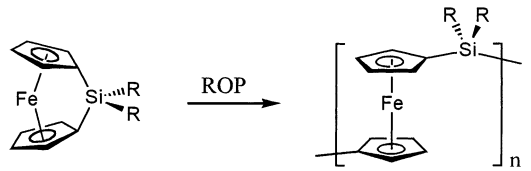

1 **2**

Scheme 2

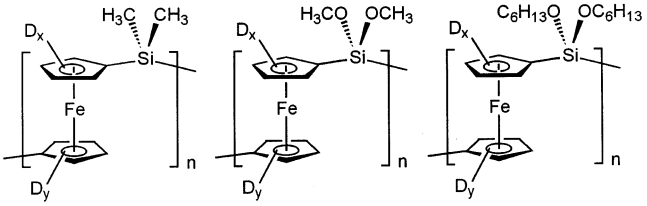

x = y ≈ 4 x = y ≈ 4 x = y ≈ 4

2a **2b** **2c**

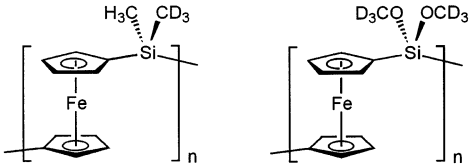

2d **2e**

Scheme 3

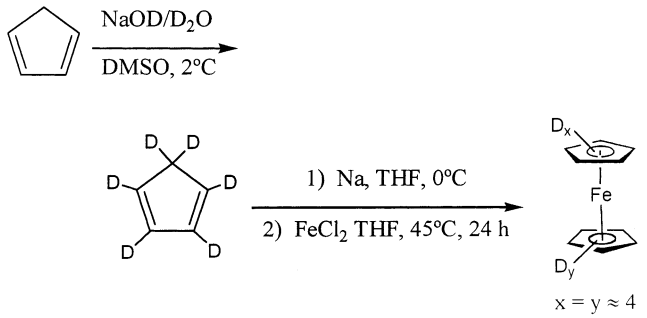

x = y ≈ 4

Results

Synthesis and Characterization of Selectively Deuterated PFSs 2a−e. Deuterio-labeling of specific sites within a polymeric material allows the mobility of different segments to be studied independently by variable temperature solid-state deuterium NMR. In the case of PFS derivatives we were able to adapt previously developed synthetic pathways in order to introduce deuterium labels in high concentration either to the cyclopentadienyl rings of the ferrocene units or to the side groups attached to silicon (Schemes 1 and 2).

Selective deuteration of the ferrocene moieties present in the PFS main chain was achieved using deuterated ferrocene as the starting material. This species was prepared via a modification of the methods developed by Hamon and co-workers[37] which involved exchange of the protons of cyclopentadiene for deuterons using a triphasic reaction mixture comprised of DMSO, cyclopentadiene, and a solution of NaOD in D_2O (see Scheme 3). The deuterated product, cyclopentadiene-d_6, was then used to synthesize deuterated ferrocene, with

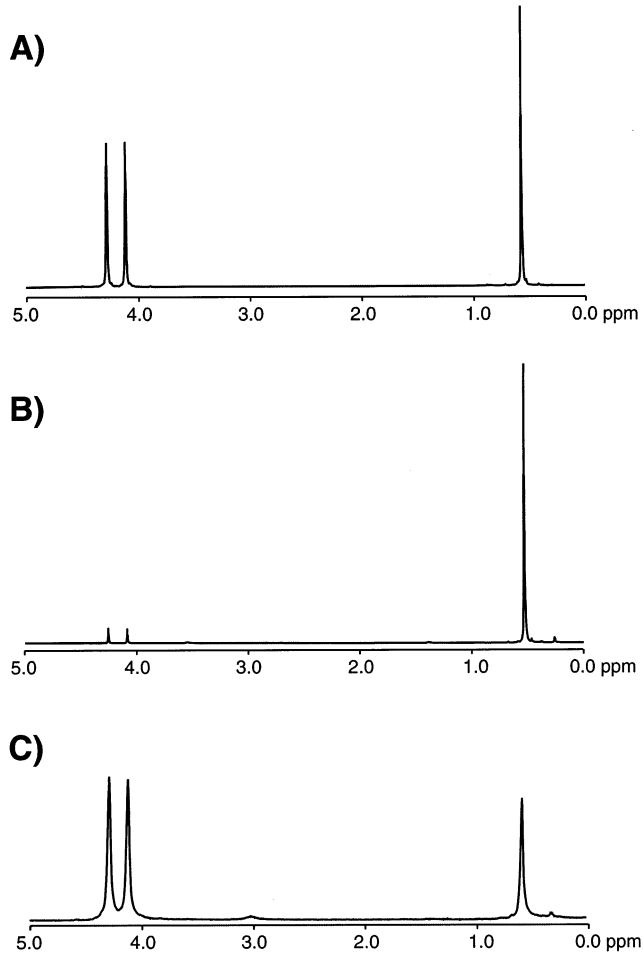

Figure 1. Solution ^{1}H NMR spectra of three different poly-ferrocenyldimethylsilanes: (A) nondeuterated poly(ferrocenyldimethylsilane), (B) ferrocene-deuterated poly(ferrocenyl-d_8-dimethylsilane), **2a**, and (C) methyl-deuterated poly(ferrocenyldimethyl-d_3-silane), **2d**. Reduction in the intensity of resonances relative to the nondeuterated case results from the deuteration of the cyclopentadienyl ligands in **2a** and one of the two methyl groups in **2d**.

approximately 95% deuteration of the Cp−H sites by mass spectrometry. The selectively cyclopentadienyl-deuterated silicon-bridged ferrocenophane monomers **1a**−**1c** were then synthesized according to literature procedures via dilithiation and subsequent treatment with chlorosilanes.[5,6] Direct ROP or substitution of the Si−Cl bonds in the monomers followed by ROP were used to prepare the PFSs **2a**, and **2b**,**c**, respectively. The degree of deuteration in **2a**−**c** was estimated from solution ^{1}H NMR to be in excess of 90%. The ^{1}H NMR spectra in Figure 1a for the nondeuterated poly(ferrocenyldimethylsilane) can be directly compared with the deuterated analogue, **2a**, shown in Figure 1b to estimate the degree of substitution. The peaks corresponding to the α- and β-protons of the Cp ligands, near 4.1 and 4.2 ppm, show a 94% decrease in intensity due to the high level of deuteration.

The selective deuteration of the side groups at silicon was achieved by two different synthetic methods. The first strategy utilized direct halide substitution[38] on poly(ferrocenylchloromethylsilane) with Me-d_3 Li in THF to form the methyl-deuterated polymer **2d** (see Scheme 4). The second strategy involved the reaction of methanol-d_4 with the $SiCl_2$-bridged monomer in the presence of an HCl acceptor, followed by ROP to form

Scheme 4

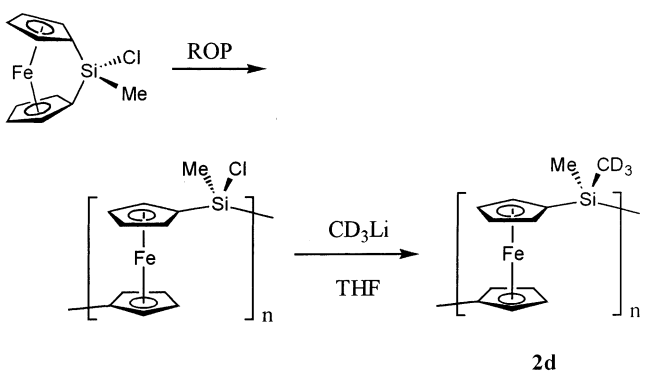

2d

Scheme 5

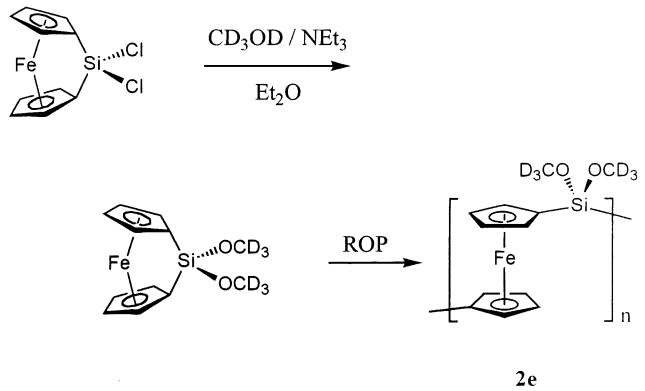

2e

2e using a procedure analogous to that recently reported for the nondeuterated counterpart (see Scheme 5).[34] Analysis of the ^{1}H NMR spectra for **2d** and **2e** showed that, within the detection limit of the experiment, the chlorine substituents had been substituted with CD_3 or OCD_3 groups, respectively. This is illustrated by a comparison of the spectra in Figure 1a,c where in the latter the expected 50% reduction in the intensity of the methyl resonance near 0.6 ppm for the deuterated PFS, **2d**, is apparent. The high molecular weight nature of each of the PFSs **2a**−**e** was confirmed by GPC analysis.

Solid-State ^{2}H NMR of PFSs with Deuterated Ferrocene Groups. Selectively ferrocene-deuterated PFSs were examined in order to probe motions of the polymer backbone as a function of temperature relative to T_g for the three different polymers **2a**, **2b**, and **2c**.

At 0 °C, the ^{2}H NMR spectrum of poly(ferrocenyl-d_8-dimethylsilane), **2a**, shown in Figure 2, upper row, consisted of a Pake doublet powder pattern with an asymmetry parameter near zero and a quadrupolar splitting of 131 kHz, slightly less than that of static ferrocene-d_{10} (145 kHz).[39] Thus, at a temperature below the mechanical T_g the Cp ligands appear to be virtually static on the time scale of the experiment.[31] Heating produced a relatively minor change in spectral line shape, but a substantial decrease in spectral intensity, with an intensity minimum being reached at ca. 100 °C. The fact that only minor line shape changes are observed indicates that any motions present must be of relatively small amplitude. The presence of an intensity minimum is indicative of motions occurring at rates on the order of the inverse of the echo time τ in the quadrupolar echo experiment (in this case $\tau = 55$ μs, $1/\tau = 18$ kHz). Increasing the temperature to 125 °C produced a ^{2}H NMR spectrum consisting of a superposition of a broad spectral component with a

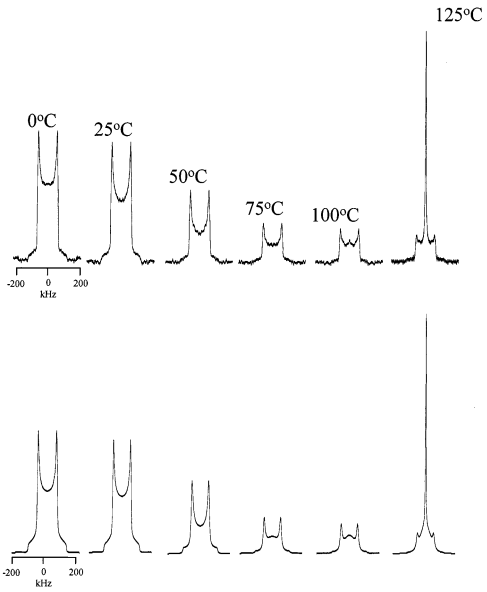

Figure 2. Experimental (upper) and simulated (lower) ^{2}H NMR spectra of poly(ferrocenyl-d_8-dimethylsilane), **2a**. The sample temperature is indicated in the figure. Simulations were performed as described in the text using the average cone angles, jump rates, and distributions shown in Figure 6.

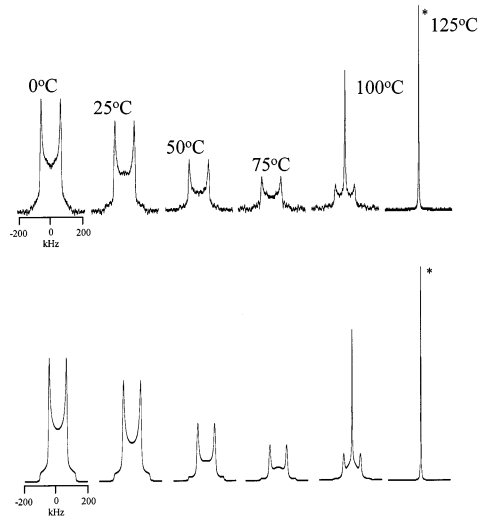

Figure 3. Experimental (upper) and simulated (lower) ^{2}H NMR spectra of poly(ferrocenyl-d_8-dimethoxysilane), **2b**. The sample temperature is indicated in the figure. Spectra marked with an asterisk (*) have been reduced in height by a factor of 10. Simulations were performed as described in the text using the average cone angles, jump rates, and distributions shown in Figure 6.

narrow isotropic resonance. The latter indicates the presence of fast large-amplitude motions about all axes simultaneously.

The ^{2}H NMR spectrum of poly(ferrocenyl-d_8-dimethoxysilane), **2b**, at 0 °C likewise consisted of a Pake doublet powder pattern with an asymmetry parameter near zero and a quadrupolar splitting of 133 kHz, as shown in Figure 3, upper row. Hence, the Cp rings of **2b** also appear static at temperatures below the polymer's mechanical T_g. Upon heating, the spectral line shape displayed minor changes, while the spectral intensity decreased substantially, reaching a minimum near 75 °C. The latter, again, is indicative of rates of motion approaching 18 kHz. At 100 °C the ^{2}H NMR spectrum consisted of superimposed broad and isotropically narrow components. At 125 °C, only the isotropic resonance remained.

The ^{2}H NMR spectra of poly(ferrocenyl-d_8-dihexyloxysilane), **2c**, as a function of temperature are shown in Figure 4, upper row. At −50 °C, i.e., at a temperature near the mechanical T_g, the spectrum was characteristic of virtually static Cp rings, as found at similar temperatures with respect to T_g for polymers **2a** and **2b**. With increasing temperature the spectral line shape of polymer **2c** underwent relatively minor changes but displayed a substantial decrease in intensity, mirroring the effects observed with polymers **2a** and **2b**. Likewise, at a temperature roughly 50 °C above T_g there was a transition over a narrow temperature range to an isotropic resonance line. The latter increased in intensity with increasing temperature.

The changes in ^{2}H NMR spectral line shape and intensity observed here with ferrocene-deuterated PFSs as a function of temperature indicate that near T_g the ferrocene rings experience only relatively slow motions of small amplitude. Increasing temperature caused spectral changes consistent with a progressive increase in both the rate and the amplitude of motion until, over a relatively narrow temperature range in the region of 50−70 °C above T_g, the motional regime transformed to one characterized by rapid isotropic averaging.

The temperature relative to T_g, rather than absolute temperature, appears to be the determining factor here. This is evident from Figure 5A in which spectral intensity is plotted vs the reduced temperature $T - T_g$ for all three ferrocene-deuterated PFSs. Despite the large differences in T_g among **2a**, **2b**, and **2c**, all three intensity curves reach a minimum at the same temperature relative to the respective mechanical T_g. This agrees well with findings in organic polymer systems for which the NMR-defined T_g is generally 60−80 °C higher than the mechanical T_g.[31e] The intensity minimum itself is diagnostic of the presence of motions with correlation times on the order of the echo time in the quadrupolar echo pulse sequence used to obtain the ^{2}H NMR spectra (i.e., 55 μs for **2a,b** and 30 μs for **2c**). However, the spectral intensity loss for the semicrystalline polymers **2a** and **2b** appears to be less dramatic than that measured for the amorphous polymer **2c** and occurs over a broader temperature range, indicating that significant differences exist between the motions present in the semicrystalline and amorphous polymers.

To obtain further insight into the nature of the motions present in these polymers, inversion−recovery T_1 relaxation time measurements were performed on **2c**, where a significant range of temperatures both below and above the intensity minimum were accessible. At all temperatures the spin−lattice relaxation could be described by a single-exponential decay. Values of T_1 decreased with increasing temperature, from roughly 200 ms at the lowest temperature to roughly 10 ms at the highest temperature. This indicates that $\tau_c\omega_0 > 1$, where τ_c is the correlation time for molecular motion and ω_0 is the Larmor frequency. The activation energy for the motions contributing to the T_1 relaxation in the higher temperature range, i.e., above the intensity minimum, could be estimated using an Arrhenius type relationship, which yielded a value of 7.5 kJ mol^{-1}. There were too few data points in the lower temperature range to obtain a reliable estimate of the activation energy at temperatures below the intensity minimum.

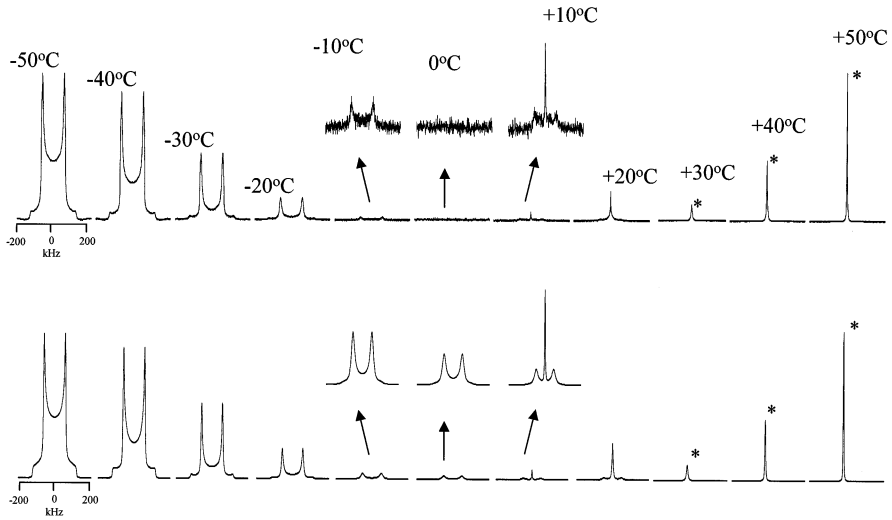

Figure 4. Experimental (upper) and simulated (lower) ^{2}H NMR spectra of poly(ferrocenyl-d_8-dihexyloxysilane), **2c**. Spectra marked with an asterisk (*) have been reduced in height by a factor of 10. Simulations were performed as described in the text using the average cone angles, jump rates, and distributions shown in Figure 6.

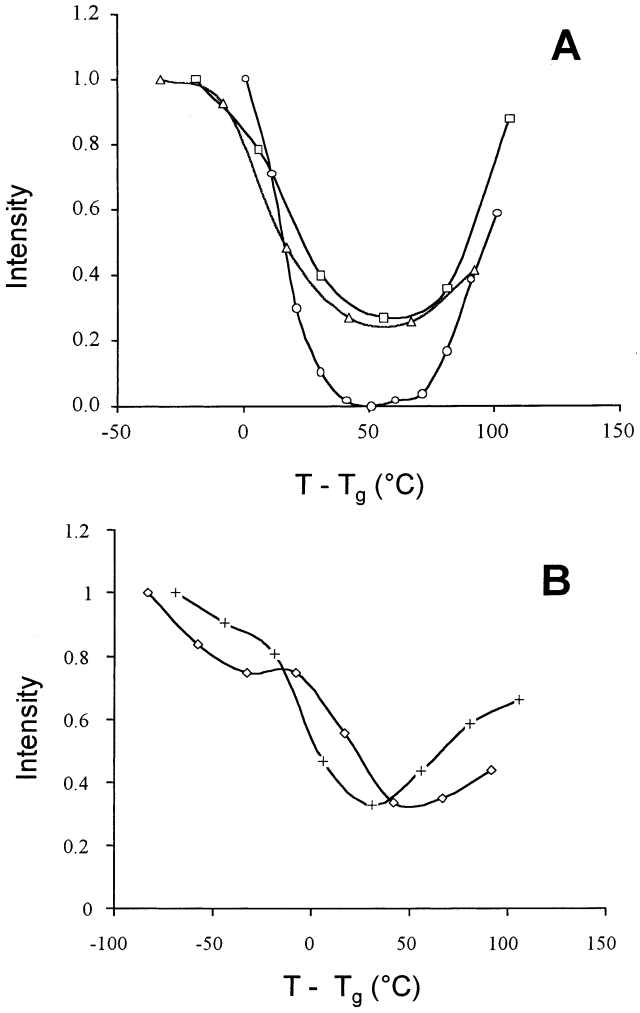

Figure 5. Relative intensities of ^{2}H NMR spectra as a function of temperature relative to T_g: (A) polyferrocenysilanes **2a** (squares), **2b** (triangles), and **2c** (circles); (B) polyferrocenylsilanes **2d** (diamonds) and **2e** (crosses). Integrated spectral intensities were normalized relative to that of the lowest temperature spectrum acquired for a given polymer.

Simulation of Ferrocene-d_8 Polyferrocenylsilane ^{2}H NMR Spectra. The sensitivity of ^{2}H NMR line shapes to the details of molecular motions affords the opportunity to extract particulars regarding the types of motion present, as well as their amplitudes and rates, using spectral simulations. The ^{2}H NMR spectral simulations program developed by the Volds[36] is widely used for this purpose and is adopted here.

Qualitatively, the ^{2}H NMR spectra of **2a**, **2b**, and **2c** at temperatures near and just above T_g indicate the presence of relatively slow, small-angle oscillations of the C−D bonds about their equilibrium positions. A simple model to simulate random oscillations about an average position is that described by Greenfield et al.[33] in which the C−D bond is permitted to "wobble" within a cone. The simulation involves jumping of the C−D bond between its equilibrium orientation, lying along the principal axis of the cone, and a number of sites (typically 8) distributed evenly on the surface of the cone. The amplitude of oscillation then corresponds to the cone angle.

Such a model, incorporating a single jump rate and a single cone angle, yielded reasonable simulations of the temperature-dependent line shape and intensity changes observed experimentally in Figures 2−4, simply by increasing the jump rate and cone angle with increasing temperature.

Molecular dynamics in glassy solids, such as those formed by PFSs, are more accurately described, however, in terms of a distribution of correlation times.[31h] Thus, a significant improvement in the quality of the fit between simulated and experimental spectral line shapes, as assessed from the frequency-weighted root-mean-square difference between the two, was achieved by assuming a Gaussian distribution of jump rates and cone angles about an average value corresponding to the best fit from the single jump rate and cone angle simulations. To simulate such a distribution of jump rate and cone angle, a composite spectrum was generated consisting of five components corresponding to the average value, $\pm\sigma$ and $\pm 2\sigma$, where σ refers to the standard deviation of the Gaussian distribution. The jump rate and cone angle were assumed to increase/decrease in tandem, as indicated by the earlier single jump rate and cone angle simulations. The components were summed with weighting coefficients corresponding to the integrated areas under a normalized Gaussian over the intervals $-^1/_2\sigma$ to $+^1/_2\sigma$, $+^1/_2\sigma$ to $^3/_2\sigma$, and $^3/_2\sigma$

to $^5/_2\sigma$, as calculated using the error function. Subdividing the Gaussian distribution into a greater number of components (i.e., 7 or 9) produced no further improvement in the quality of the fit of simulations to experimental spectra.

It was likewise possible to simulate the experimental spectra using a model in which the C−D bond wobbled within an elliptic cone, rather than a circular cone. Such a model implies a preferential direction of oscillation along some particular axis, corresponding to the major axis of the elliptic cone. The resulting simulations, even for large eccentricities (i.e., 10:1 ratio of angular excursions along the major vs minor axis of the ellipse), produced simulated spectra with line shapes only subtly different from those produced by assuming wobbling within a circular cone. The differences were too marginal to allow any decision between the two situations on the basis of comparison with experimental spectra.

The similarities between the spectral simulations obtained from assuming wobbling in a circular vs an elliptic cone arise from the fact that the ferrocene deuterons possess an asymmetry parameter η close to zero.[31f,32] Hence, motions of the C−D bond influence the effective quadrupolar Hamiltonian only through the polar angle θ, describing the degree of off-axis wobble of the C−D bond, and not through the azimuthal angle ϕ, describing any degree of preference for a particular direction of wobble. Since the circular cone model is simpler than the elliptic cone model (requiring that one specify only one rather than two cone angles), it was adopted exclusively.

At temperatures well above T_g an isotropically narrow spectral component is observed in all cases, superimposed upon the broad underlying spectral component and increasing in intensity with increasing temperature. We associate this component with amorphous regions of the sample wherein individual polymer segments experience thermally activated, rapid, large-amplitude motions producing isotropic averaging. From a simulation perspective isotropic averaging is most expediently achieved by allowing the C−D bond to jump rapidly (jump rate > 50 MHz) between three sites corresponding to the three axes of a Cartesian coordinate system. The resulting isotropically narrow spectrum was incorporated into the simulations as a second and separate spectral component, the intensity of which was adjusted using a temperature-dependent weighting factor in the spirit of Vogel and co-workers.[31h]

The success of this approach to simulating the experimental ^{2}H NMR spectra is clear from a comparison of the simulated and experimental spectra in Figures 2−4. To properly simulate the changes in line shape and intensity with increasing temperature required a progressive increase in the average jump rate and the average cone angle, as detailed in parts A and B of Figure 6, respectively. These changes were combined with a broadening of the distribution about the average values with increasing temperature, likewise illustrated in Figure 6.

Figure 6 permits a comparison for the three polymers of the overall extent of C−D bond motion. In all cases, below T_g only small angular excursions from equilibrium occur, and rates of motion are slow. Above T_g angular excursions increase progressively in amplitude and rate with increasing temperature. This reflects the dominant role played by T_g in determining the degree

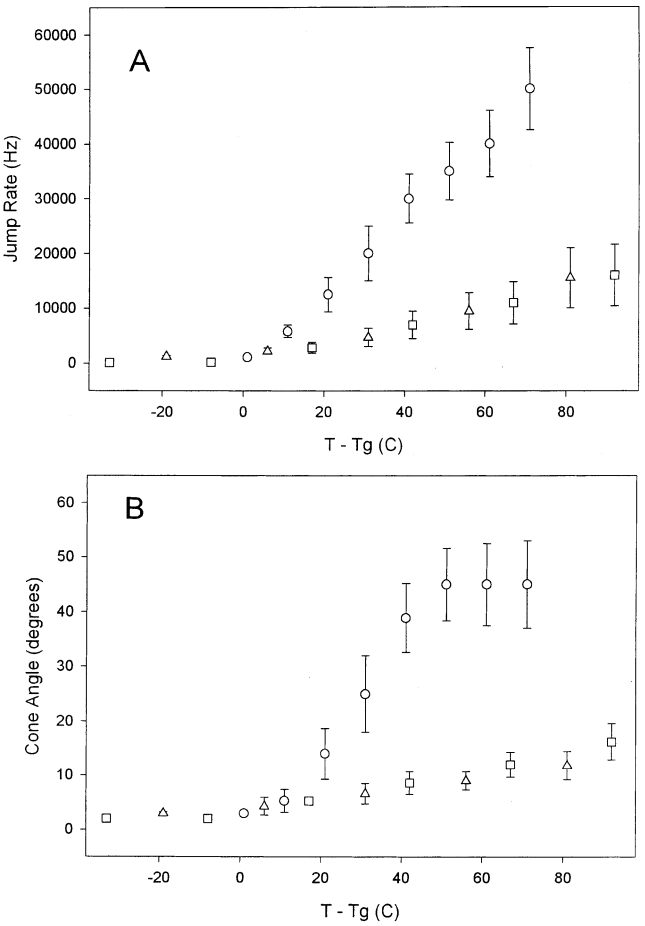

Figure 6. (A) Average jump rate for C−D bond motion in polyferrocenylsilanes **2a** (squares), **2b** (triangles), and **2c** (circles) as a function of temperature relative to the respective T_g. Jump rates were obtained from spectral simulations of corresponding ^{2}H NMR spectra using a motional model in which the C−D bond is permitted to wobble within a cone. It is further assumed that the sample is heterogeneous with a Gaussian distribution of possible jump rates about the average. Bars indicate the optimal breadth of the distribution of jump rates and correspond to one standard deviation within the assumed Gaussian distribution. (B) Average cone angle for C−D bond motion in polyferrocenylsilanes **2a** (squares) **2b** (triangles), and **2c** (circles) as a function of temperature relative to the respective T_g. Cone angles were obtained from spectral simulations as described above and in further detail in the text. Bars indicate the optimal breadth of the distribution of jump rates and correspond to one standard deviation within the assumed Gaussian distribution.

of motional freedom in polymer systems in general. Nevertheless, significant differences between the three PFSs now become evident. In particular, the amplitude and rate of Cp oscillations increased in the order **2a** < **2b** ≪ **2c**, which is precisely the inverse order of the T_g's of these three polymers.

Activation energies for the motions contributing to the observed line shape changes may be calculated from the temperature dependence of the jump rates obtained by simulation, assuming the usual Arrhenius relation. In the higher temperature range, where a comparison of all three PFSs is possible, the activation energy equaled 24.8 kJ mol^{-1} for polymer **2a**, 21.7 kJ mol^{-1} for polymer **2b**, and 11.9 kJ mol^{-1} for polymer **2c**. The latter value compares favorably with the activation energy calculated for this polymer from the temperature dependence of the T_1 values. The comparison between the three PFSs demonstrates that the activation energy decreases

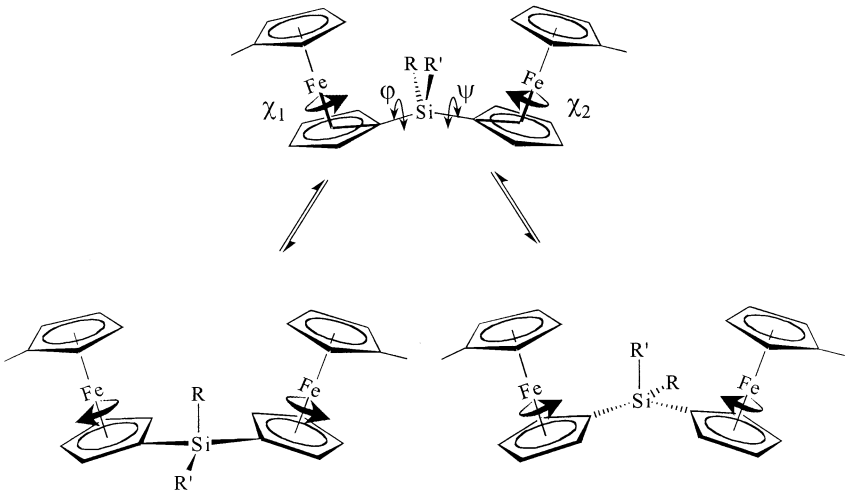

Figure 7. Schematic showing the torsion angle nomenclature of Barlow et al.[8] and the proposed "coupled Cp ring torsion" model derived from the ^{2}H NMR spectra of ferrocene-deuterated polyferrocenylsilanes.

in the order **2a** > **2b** ≫ **2c**, which is precisely the order of the T_g's of these three polymers.

In summary, the ^{2}H NMR studies of **2a**, **2b**, and **2c** reveal that, in all cases, below T_g the Cp rings of the PFS backbone undergo only slow, small-amplitude motions about their equilibrium positions. Above T_g, in all cases, the Cp rings begin to experience increased rates and amplitudes of torsional flexing. At approximately 50 °C above the respective T_g in all cases there is an abrupt transition to a phase characterized by fast isotropic motional averaging of the PFS backbone. In the temperature region 0 °C < $T - T_g$ < 50 °C, significant differences between the different PFSs are evident, in that the lowest T_g polymer **2c** exhibited the highest rates and amplitudes of backbone torsional flexing and the lowest activation energy for these motions.

A Model of Polyferrocenylsilane Backbone Motions in the Region $T_g < T < T_m$. At temperatures below T_g ^{2}H NMR indicates that the PFS backbone is virtually static, constrained as it is by interpolymer chain packing considerations. At temperatures approaching T_m ^{2}H NMR shows that the backbone enjoys virtual isotropic motional freedom, at least at the segmental level, due to alleviation of interpolymer chain packing constraints. To understand the motions present in the polymer backbone at temperatures between these two extremes, it is necessary to link the C−D bond motions indicated by ^{2}H NMR to possible, or likely, motions of the PFS backbone.

It is convenient, therefore, to introduce the dihedral torsion angles defined by O'Hare and co-workers[8] and shown schematically in Figure 7. The torsion angle φ refers to the rotation of one ferrocene about the bond to the bridging silicon atom, while ψ describes the rotation of the second ferrocene about its bond to the bridging silicon. Any oscillation about φ or ψ involves displacing an entire ferrocene unit, unless coupled with some compensatory torsioning elsewhere along the polymer backbone. Another dihedral angle χ describes the rotation of one Cp ring relative to the other within the same ferrocene unit. In ferrocene, individual Cp rings enjoy virtually free rotation, and rapid rotation is observed down to −193 °C.[40] However, in PFS the preferred value of χ is generally close to 180° due to polymer packing constraints.[7−9] Any torsioning about the preferred value of χ would involve displacing an entire neighboring ferrocene unit, unless coupled with some compensatory torsioning elsewhere along the polymer backbone. A further possible oscillation, not specifically considered by O'Hare and co-workers,[8] involves tilting of the two Cp rings of ferrocene with respect to one another. However, the two Cp rings are normally coplanar, and the activation barrier to ring tilts greater than roughly 13° is prohibitive.[41] Hence, if present, the Cp ring tilt will be constrained to small angles only.

Any proposed motional model must have activation barriers sufficiently low as to permit Cp ring oscillations of the amplitude indicated from the ^{2}H NMR spectra. One example is the "coupled Cp ring torsion" model shown schematically in Figure 7.[42] It involves coupled clockwise/anticlockwise rotations of the two Cp rings on neighboring ferrocenyl units linked by a bridging silicon atom. This corresponds to changes of opposite sign in the torsion angles χ_1 and χ_2, respectively, where the subscripts refer to the adjacent ferrocenyl units. Consequent to this motion, the two torsion angles φ and ψ also change, but again in a coupled manner and in an opposite sense.

The drivers in this motional model are the Cp ring rotations, a motion known to have a low activation barrier in ferrocene.[30] By coupling rotation of one Cp ring to that of its silicon-bridged neighbor, no ferrocenyl displacement results, the free volume required is relatively small, and the activation barrier is minimized. The major displacement occurs at the silicon atom, whose side groups sweep through an arc corresponding to the torsion angle about χ. The free volume requirements for silicon side group motions are clearly less than for ferrocene motions, at least for the particular side groups of concern here. The fact that the model avoids displacement of entire ferrocenyl units means that the motions can occur locally, at the segment level, with little disruption of polymer chain packing.

Coupled Cp ring torsioning about χ produces an oscillatory motion of the C−D bonds within the plane of the Cp rings, having minimal free volume requirements. Uncoupled torsioning about any of φ, ψ, or χ, on the other hand, or tilting of one Cp ring with respect to the other in a given ferrocene, produces out-of-plane oscillations of a Cp ring C−D bond, having relatively large free volume requirements. Coupled oscillations of pairs of ferrocene units bridged by a silicon atom are also conceivable, but inevitably involve greater free

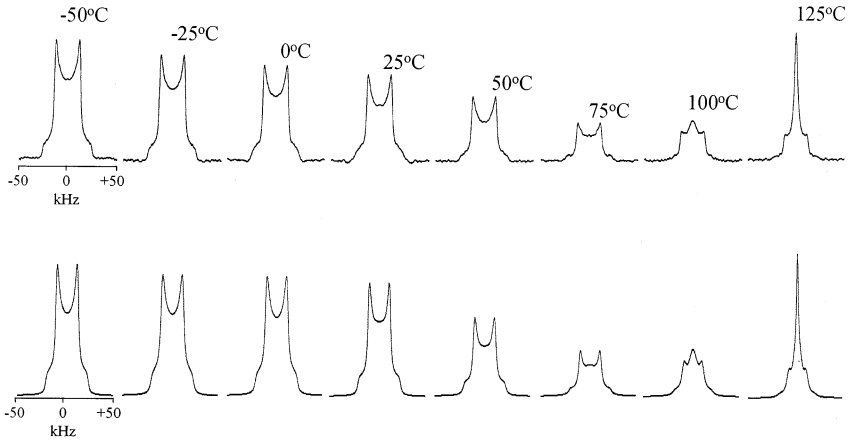

Figure 8. Experimental (upper) and simulated (lower) ^{2}H NMR spectra of poly(ferrocenyldimethyl-d_3-silane), **2d**. Details of the simulation parameters used are provided in the text.

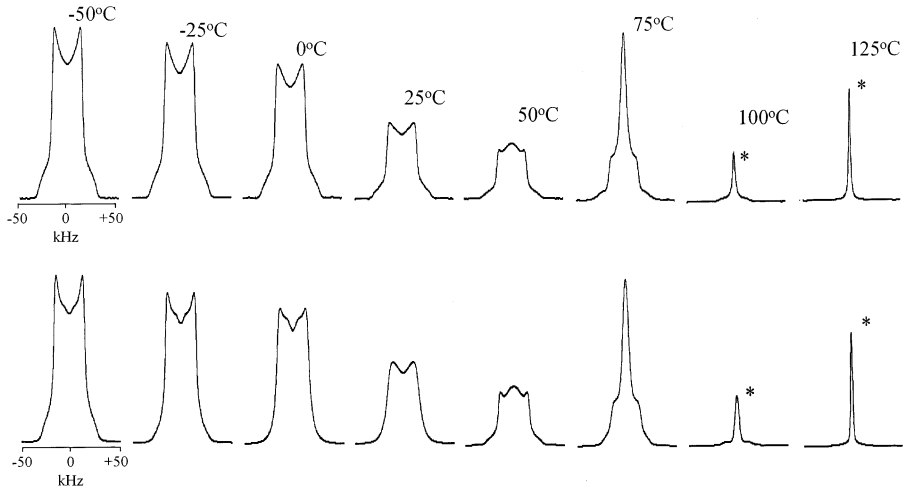

Figure 9. Experimental (upper) and simulated (lower) ^{2}H NMR spectra of poly(ferrocenyldimethoxy-d_6-silane), **2e**. Spectra marked with an asterisk (*) have been reduced in height by a factor of 10. Details of the simulation parameters used are provided in the text.

volume requirements that the coupled Cp ring torsioning of pairs of Cp rings joined by a bridging silicon. Hence, we conclude that the "coupled Cp ring torsion" model proposed here is the simplest model consistent with the ^{2}H NMR data.

Solid-State ^{2}H NMR of Polyferrocenylsilanes with Deuterated Silicon Side Groups. ^{2}H NMR spectra of methyl-deuterated poly(ferrocenyldimethylsilane), **2d**, and methoxy-deuterated poly(ferrocenyldimethoxysilane), **2e**, were examined over a range of temperatures (−50 to +125 °C) spanning the mechanical T_g in order to probe side chain motions occurring in addition to the backbone motions examined above.

For polymer **2d** (T_g = 33 °C) at −50 °C, the ^{2}H NMR spectrum, as shown in Figure 8, consisted of a Pake doublet powder pattern with an asymmetry parameter near zero and a quadrupolar splitting of 40 kHz. This is the value expected for fast rotation of the methyl group about the Si−CD_3 bond, so that no additional motions of the polymer backbone need to be invoked to explain this spectrum. This is in accord with the finding above that the ferrocene units of this polymer are virtually static below the mechanical T_g. With increasing temperature the spectra of polymer **2d** changed little in line shape, but decreased in intensity, reaching an intensity minimum at roughly 50−60 °C above T_g. Details of the temperature dependence of the spectral intensity for **2d** are shown in Figure 5B. At 100 °C, the spectrum consisted of a superposition of a broad component and an isotropically narrow spectral component. The latter increased in relative intensity as the temperature was raised further to 125 °C. In many respects, therefore, the ^{2}H NMR spectra from methyl-deuterated poly(ferrocenyldimethylsilane) exhibit temperature-dependent features similar to those of the corresponding ferrocene-deuterated polymer **2a**. Clearly, the backbone motions of the polymer are being superimposed upon the motions experienced by the silicon side chains. The latter, in this case, is simply fast methyl rotation.

As shown in Figure 9, for polymer **2e** (T_g = 19 °C) the ^{2}H NMR spectrum at −50 °C consisted of a Pake powder pattern with a quadrupolar splitting of 33 kHz. This is smaller than one would predict if the only motion present was fast rotation of the methyl group about the O−C bond. Since the corresponding ferrocene-deuterated polymer **2b** exhibits only slow, small-amplitude ring oscillations, backbone motion cannot be a significant contributor to this decrease in quadrupolar splitting. It is likely, therefore, that motions about the Si−O bond of the methoxy side chain contribute to this decrease, a notion which can be addressed by spectral simulation (see below). With increasing temperature the spectra of polymer **2e** showed few line shape changes but decreased in intensity and, as observed in all other

cases, reached an intensity minimum at roughly 50−60 °C above T_g. Details of the temperature dependence of the spectral intensity for **2e** are shown in Figure 5B. At both 75 and 100 °C, the spectrum consisted of a superposition of a broad component and an isotropically narrow spectral component, the latter increasing in relative intensity with increasing temperature.

Hence, the ^{2}H NMR spectra from methoxy-deuterated poly(ferrocenyldimethoxysilane) also exhibit temperature-dependent features similar to those of the corresponding ferrocene-deuterated polymer, so that backbone motions are apparently being superimposed upon the motions experienced by the silicon side chains. The latter, in this case, involve more than simply fast methyl rotations.

Simulation of ^{2}H NMR Spectra of PFS Deuterated Side Groups. The experimental ^{2}H NMR spectra reflect a superposition of backbone and side group motions in the PFSs. For poly(ferrocenyldimethylsilane) the minimal side group motion is fast methyl rotation. The issue then concerns what additional motion is introduced at the side group by the type of Cp ring oscillation observed for polymer **2a** and whether the corresponding average rate and amplitude of ring oscillation, and the width of their distribution, suffice to explain the temperature dependence of the side group spectra observed for polymer **2d**.

As shown schematically in Figure 7, the coupled Cp ring torsion model describing backbone motions causes the methyl groups to rotate through an arc of length dictated by the amplitude of in-plane Cp ring oscillations. This motion is modeled as a wobbling of the methyl group within a cone.

Figure 8 shows the simulated ^{2}H NMR spectra for polymer **2d** based on the motional model described above. It is evident that the temperature dependence of the line shapes and intensities of the ^{2}H NMR spectra of methyl-deuterated poly(ferrocenyldimethylsilane) are reproduced with high fidelity using the coupled Cp ring torsion model. However, the rate and amplitude of Cp ring oscillation yielding the best fit between experiment and simulation for polymer **2d** were generally somewhat greater, and the distribution about the averages somewhat broader, than those obtained with polymer **2a**. The discrepancies can be attributed either to uncertainties in the quality of the fit or to differences in polymer thermal history.

Turning to methoxy-deuterated poly(ferrocenyldimethoxysilane), we note that the ^{2}H NMR spectra of polymer **2e** indicate that its methoxy side groups experience fast methyl rotation about the O−Me bond plus additional motional averaging. Simulations incorporating the coupled Cp ring torsion motions deduced from examination of polymer **2b** as the only additional motion experienced by the methoxy side group failed to satisfactorily reproduce the experimental ^{2}H NMR spectra in Figure 9.

Successful simulations were produced, however, when consideration was taken of motions occurring about the Si−O bond of the methoxy side group. These were modeled as restricted rotational isomerizations, akin to the restricted trans−gauche isomerization observed in polymethylene chains in condensed media.[43] As the Newman projection along the O−Si bond in Scheme 6 illustrates, there are three possible rotational conformers for which the methyl group is in a staggered conformation with respect to the substituents on the

Scheme 6

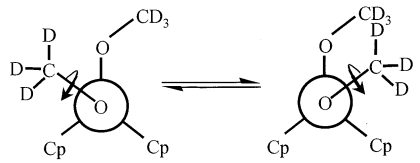

silicon atom. Simulations were conducted incorporating discontinuous jumps of the methyl group between these lowest-energy, symmetry-related sites, assuming a near-tetrahedral Si−O−Me bond angle.[44] Backbone motions were included by assuming the same coupled Cp ring torsion model described above for the case of the methyl side groups. The jump rate between rotational conformers was equal to the rate of oscillation of the Si−O bond, and the latter rate, in turn, was found to be identical to the rate of Cp ring oscillation deduced for polymer **2b**. Hence, there is an obvious coupling between backbone and side group motions. The simulations were found to be sensitive particularly to the a priori population of the three methoxy rotational conformers and the jump rate between them. Specifically, only two sites were significantly populated, and their a priori populations were 85/15. Simulations employing 90/10 or a 80/20 a priori populations were clearly inferior in quality of fit to the experimental spectrum. One may rationalize this restricted rotational isomerization as arising from differences in steric hindrance among the three rotational conformers. Defining the C−O−Si−O torsion angle α in Scheme 6 as equal to 0° when the methoxy groups are eclipsed, the rotational conformer having $\alpha = 180°$, which places the methoxy group between the two Cp substituents, is clearly the most restrictive sterically and can be considered not populated. This applies to both methoxy groups. The remaining two rotational conformers may be differentiated on the basis of whether the two methyl groups are distal or proximal, the latter being sterically unfavorable.

In summary, the ^{2}H NMR studies of polymers **2d** and **2e** reveal that, in both cases, side group motions reflect a combination of backbone-dependent and backbone-independent motions. Backbone-independent motions include fast methyl rotations, which occur even at temperatures far below the particular T_g. Backbone-dependent motions appear to consist of rotational oscillations within the R−Si−R plane (R = Me or OMe), resulting from coupled in-plane ring oscillations occurring on the two Cp rings bridged by the silicon atom. For the methoxy side groups, coupling between backbone and side group motions extends to the case of rotational isomerization about the Si−O bond.

Discussion

The main objectives of this work were to characterize the types of motion undergone by the backbone and side groups of PFSs, to quantify their rates and amplitudes as a function of temperature, and to examine any differences between three specific PFSs.

All of the polymers examined here appear to undergo restricted torsioning of their Cp rings about the torsion angle χ as embodied by the coupled Cp ring torsion model proposed here to explain the observed temperature-dependent ^{2}H NMR spectral features. While it is likely that out-of-plane Cp rings motions also occur, and the ^{2}H NMR spectral simulations do not directly differentiate in-plane vs out-of-plane Cp ring motions;

nevertheless, the dominant spectral characteristics were reproduced using a single type of motion and a single effective correlation time.

It is undoubtedly true that other, more complicated, motional models might be proposed to explain the ^{2}H NMR spectral features observed here. The glass transition, for example, generally involves cooperative motions of extended segments, while our proposed model involves only highly localized motions. Moreover, the present model does not take into account deviations of bond angles from their equilibrium values: the Si−O−CD_3 bond angle, for example, is quite flexible.[44]

Nevertheless, many points support the coupled Cp ring torsion model including its consistency with the calculations of O'Hare,[8] its exploitation of the known low activation barrier to rotations about the Fe−Cp centroid,[30] and, not least, its success in explaining both backbone and silicon side group motions in three different types of PFS. This suggests that, at a minimum, this motional model provides a good basis for further study of these metal-containing polymers. In particular, 2D ^{2}H NMR exchange spectroscopy might prove useful in elucidating more exactly the nature of the motions undergone by the backbone and silicon side groups of PFSs.

The current studies have brought to light clear differences in the relative mobility of the semicrystalline polymers **2a,d** and **2b,e** compared to the amorphous polymer **2c**, even when compared at corresponding temperatures relative to T_g. For example, the semicrystalline polymers **2a,d** and **2b,e** exhibit ^{2}H NMR spectra with superimposed broad and narrow spectral components at temperatures above the respective mechanical T_g. This indicates that semicrystalline regions of the sample, having a closer packing of polymer chains and a reduced free volume, resist the effects of increasing temperature on motional rates and amplitudes, compared to more amorphous regions. It is not at all unusual, given the heterogeneous nature of polymeric materials, to find variations in backbone and side group environments that may be modeled in terms of a distribution of rotational rates and amplitudes.[31] For an amorphous polymer (**2c**) the distinctions between regions within the sample are less sharply drawn, and the ^{2}H NMR spectra reflect a more homogeneous environment across the sample. Overall, the amorphous polymer (**2c**) exhibited a higher mobility than its semicrystalline counterparts, in terms of both rates and amplitudes of motion. This is a reflection of the less dense chain packing resulting from the larger hexyloxy silicon side groups of **2c** relative to the methyl or methoxy side groups of **2a** and **2b**. In all cases, isotropic motion was observed at temperatures 50−60 °C above the respective mechanical T_g. However, for the semicrystalline polymers, complete conversion to the isotropic regime did not occur until above the melt, as is observed with organic polymers.

Summary

Solid-state deuterium NMR has provided unique insight into the molecular motions present in PFSs with alkyl or alkoxy substituents at silicon. At temperatures near or below T_g, PFSs have freely moving side groups coupled to a relatively rigid backbone. As the polymer is heated above the mechanical T_g, backbone motion occurs via a coupled rotation of two adjacent the Fe−Cp centroids with moderate amplitudes (<90°) and correlation times approaching the tens of kilohertz time scale. Intensity minima were observed at temperatures well above their mechanical T_g (50−70 °C), consistent with behavior observed with organic polymers. At higher temperatures the polymer backbone abruptly begins to undergo essentially isotropic motions, at least at the segmental level. The complex nature of the motions undergone by polymers **2d** and **2e** suggests that deuterium-exchange NMR experiments might be useful in better dissecting the correlation between backbone and side group contributions and to help assess the validity of the models proposed here.

Acknowledgment. We thank Dr. Hiltrud Grondey for helpful discussions, Marc Mamak for PXRD, Alison Cheng for DSC measurements, and Andrea Berenbaum for artwork. K.K. is grateful to NSERC for a Postgraduate Scholarship. I.M. thanks the Canadian Government for a Canada Research Chair in Inorganic and Polymer Chemistry, the University of Toronto for a McLean Fellowship (1997−2002), and the Ontario Government for a PREA Award (1999−2004) for the duration of the work described. P.M. gratefully acknowledges the support of NSERC Operating Funds.

References and Notes

(1) See for example: (a) Bernhard, B.; Spiess, H. W. *Angew. Chem., Int. Ed. Engl.* **1988**, *27*, 1655. (b) Rushkin, I. L.; Interrante, L. V. M*acromolecules* **1996**, *29*, 3123.
(2) (a) Spiess, H. W. *Colloid Polym. Sci.* **1983**, *261*, 193. (b) Hentschel, D.; Sillescu, H.; Spiess, H. W. *Polymer* **1984**, *25*, 1078. (c) Richter, D.; Zorn, R.; Farago, B.; Frick, B.; Fetters, L. J. *Phys. Rev. Lett.* **1992**, *68*, 71. (d) Lin, W.-Y.; Blum, F. D. *J. Am. Chem. Soc.* **2001**, *123*, 2032.
(3) For recent studies of molecular motions in inorganic polymers based on main group elements see: (a) O'Connor, R. D.; Blum, F. D.; Ginsburg, E. J.; Miller, R. D. *Macromolecules* **1998**, *31*, 4852. (b) Goward, G. R.; Kerr, T. A.; Power, W. P.; Nazar, L. F. *Adv. Mater.* **1998**, *10*, 449. (c) Zeghal, M.; Deloche, B.; Auroy, P. *Macromolecules* **1999**, *32*, 4947. (d) Valic, S.; Scotta, P.; Deloche, B. *Polymer* **1999**, *40*, 989. (e) McLoughlin, K.; Szeto, C.; Duncan, T. M.; Cohen, C. *Macromolecules* **1996**, *29*, 5475.
(4) Reviews on metal-containing polymers: (a) Nguyen, P.; Gómez-Elipe, P.; Manners, I. *Chem. Rev.* **1999**, *99*, 1515. (b) Kingsborough, R. P.; Swager, T. M. *Prog. Inorg. Chem.* **1999**, *48*, 123. (c) Manners, I. *Science* **2001**, *294*, 1664.
(5) Foucher, D. A.; Tang, B. Z.; Manners, I. *J. Am. Chem. Soc.* **1992**, *114*, 6246.
(6) (a) Manners, I. *Chem. Commun.* **1999**, 857. (b) Kulbaba, K.; Manners, I. *Macromol. Rapid Commun.* **2001**, *22*, 711.
(7) Rulkens, R.; Lough, A. J.; Manners, I.; Lovelace, S. R.; Grant, C.; Geiger, W. E. *J. Am. Chem. Soc.* **1996**, *118*, 12683.
(8) Barlow, S.; Rohl, A. L.; Shi, S.; Freeman, C. M.; O'Hare, D. *J. Am. Chem. Soc.* **1996**, *118*, 7578.
(9) Papkov, V. S.; Gerasimov, M. V.; Dubovik, I. I.; Sharma, S.; Dementiev, V. V.; Pannell, K. H. *Macromolecules* **2000**, *33*, 7107.
(10) Rasburn, J.; Petersen, R.; Jahr, T.; Rulkens, R.; Manners, I.; Vancso, G. J. *Chem. Mater.* **1995**, *7*, 871.
(11) (a) Kulbaba, K.; MacLachlan, M. J.; Evans, C. E. B.; Manners, I. *Macromol. Chem. Phys.* **2001**, *202*, 1768. (b) Calleja, G.; Carre, F.; Cerveau, G.; Corriu, R. J. P. *C. R. Acad. Sci., Ser. II: Fas. C-Chem.* **1998**, *4*, 285.
(12) Espada, L. I.; Shadaram, M.; Robillard, J.; Pannell, K. H. *J. Inorg. Organomet. Polym.* **2001**, *10*, 169.
(13) Resendes, R.; Berenbaum, A.; Stojevic, G.; Jäkle, F.; Bartole, A.; Zamanian, F.; Dubois, G.; Hersom, C.; Balmain, K.; Manners, I. *Adv. Mater.* **2000**, *12*, 327.
(14) (a) MacLachlan, M. J.; Aroca, P.; Coombs, N.; Manners, I.; Ozin, G. A. *Adv. Mater.* **1998**, *10*, 144. (b) MacLachlan, M. J.; Ginzburg, M.; Coombs, N.; Raju, N. P.; Greedan, J. E.; Ozin, G. A.; Manners, I. *J. Am. Chem. Soc.* **2000**, *122*, 3878.
(15) (a) MacLachlan, M. J.; Ginzburg, M.; Coombs, N.; Coyle, T. W.; Raju, N. P.; Greedan, J. E.; Ozin, G. A.; Manners, I. *Science* **2000**, *287*, 1460. (b) Ginzburg, M.; MacLachlan, M. J.; Yang, S. M.; Coombs, N.; Coyle, T. W.; Raju, N. P.;

Greedan, J. E.; Herber, R. H.; Ozin, G. A.; Manners, I. *J. Am. Chem. Soc.* **2002**, *124*, 2625. (c) Sun, Q.; Lam, J. W. Y.; Xu, K.; Xu, H.; Cha, J. A. K.; Wong, P. C. L.; Wen, G.; Zhang, X.; Jing, X.; Wang, F.; Tang, B. Z. *Chem. Mater.* **2000**, *12*, 2617.
(16) Kulbaba, K.; Resendes, R.; Cheng, A.; Bartole, A.; Safa-Sefat, A.; Coombs, N.; Stöver, H. D. H.; Greedan, J. E.; Ozin, G. A.; Manners, I. *Adv. Mater.* **2001**, *13*, 732.
(17) Wang, Z.; Lough, A. J.; Manners, I. *Macromolecules* **2002**, *35*, 7699.
(18) Ginzburg, M.; Galloro, J.; Jäkle, F.; Power-Billard, K. N.; Yang, S.; Sokolov, I.; Lam, C. N. C.; Neumann, A. W.; Manners, I.; Ozin, G. A. *Langmuir* **2000**, *16*, 9609.
(19) Jäkle, F.; Wang, Z.; Manners, I. *Macromol. Commun.* **2000**, *21*, 1291.
(20) Hempenius, M. A.; Robins, N. S.; Lammertink, R. G. H.; Vancso, G. J. *Macromol. Commun.* **2001**, *22*, 30.
(21) Rulkens, R.; Ni, Y.; Manners, I. *J. Am. Chem. Soc.* **1994**, *116*, 12121.
(22) Ni, Y.; Rulkens, R.; Manners, I. *J. Am. Chem. Soc.* **1996**, *118*, 4102.
(23) Gõmez-Elipe, P.; Resendes, R.; Macdonald, P. M.; Manners, I. *J. Am. Chem. Soc.* **1998**, *120*, 8348.
(24) Massey, J. A.; Power, K. N.; Manners, I.; Winnik, M. A. *J. Am. Chem. Soc.* **1998**, *120*, 9533.
(25) Massey, J. A.; Power, K. N.; Winnik, M. A.; Manners, I. *Adv. Mater.* **1998**, *10*, 1559.
(26) Cheng, J. Y.; Ross, C. A.; Chan, V. Z.; Thomas, E. L.; Lammertink, R. G. H.; Vancso, G. J. *Adv. Mater.* **2001**, *13*, 1174.
(27) Massey, J.; Winnik, M. A.; Manners, I.; Chan, V. Z.-H.; Ostermann, J. M.; Enchelmaier, R.; Spatz, J. P.; Möller, M. *J. Am. Chem. Soc.* **2001**, *123*, 3147.
(28) Power-Billard, K. N.; Manners, I. *Macromolecules* **2000**, *33*, 26.
(29) See for example: (a) Mahl, A.; Hillberg, M.; Litterst, F. J.; Pöhlmann, T.; Hübsch, C.; Nuyken, O.; Garwe, F.; Beiner, M.; Donth, E. *J. Phys.: Condens. Matter* **1998**, *10*, 961. (b) Hillberg, M.; Stieler, W.; Litterst, F. J.; Burkhardt, V.; Nuyken, O. *Hyperfine Interact.* **1994**, *88*, 137. (c) Feyerherm, R.; Litterst, F. J.; Burkhardt, V.; Nuyken, O. *Solid State Commun.* **1992**, *82*, 141. (d) Litterst, F. J.; Lerf, A.; Nuyken, O.; Alcalá, H. *Hyperfine Interact.* **1982**, *12*, 317. (e) Nienhaus, U. G.; Parak, F. *Hyperfine Interact.* **1994**, *90*, 243.
(30) (a) Li, C.; Medina, J. C.; Maguire, G. E. M.; Abel, E.; Atwood, J. L.; Gokel, G. W. *J. Am. Chem. Soc.* **1997**, *119*, 1609. (b) Haaland, A.; Nilsson, J. E. *Chem. Commun.* **1968**, *22*, 2653. (c) Bohn, R.; Haaland, A. J. *Organomet. Chem.* **1966**, *5*, 470.
(31) See for example: (a) Spiess, H. W. *Adv. Polym. Sci.* **1985**, *66*, 23. (b) Schmidt-Rohr, K.; Kulik, A. S.; Beckham, H. W.; Ohlemacher, A.; Pawelzik, U.; Boeffel, C.; Spiess, H. W. *Macromolecules* **1994**, *27*, 4733. (c) Shi, J. F.; Inglefield, P. T.; Jones, A. A.; Meadows, M. D. *Macromolecules* **1996**, *29*, 605. (d) Goward, G. R.; Kerr, T. A.; Power, W. P.; Nazar, L. F. *Adv. Mater.* **1998**, *10*, 449. (e) Schmidt-Rohr, K.; Spiess, H. W. *Multidimensional Solid-State NMR and Polymers*; Academic Press: New York, 1994; pp 236−276. (f) Spiess, H. W. *Chem. Rev.* **1991**, *91*, 1321. (g) Havlicek, I.; Ilanvsky, M.; Hrouz, J. *J. Polym. Sci., Polym Phys. Ed.* **1978**, *16*, 653. (h) Vogel, M.; Rössler, E. *J. Phys. Chem. A* **1998**, *102*, 2102.
(32) Fyfe, C. A. *Solid State NMR for Chemists*; CFC Press: Guelph, Ontario, Canada, 1987.
(33) Preliminary communication: Kulbaba, K.; Macdonald, P. M.; Manners, I. *Macromolecules* **1999**, *32*, 1321.
(34) Nguyen, P.; Stojcevic, G.; Kulbaba, K.; MacLachlan, M. J.; Liu, X. H.; Lough, A. J.; Manners, I. *Macromolecules* **1998**, *31*, 5977.
(35) Kulbaba, K.; Cheng, A.; Manners, I., unpublished results.
(36) Greenfield, M. S.; Ronemus, A. D.; Vold, R. L.; Vold, R. R.; Ellis, P. D.; Raidy, T. E. *J. Magn. Reson.* **1987**, *72*, 89.
(37) Hamon, J.-R.; Hamon, P.; Sinbandhit, S.; Guenot, P.; Astruc, D. *J. Organomet. Chem.* **1991**, *413*, 243.
(38) Zechel, D. L.; Hultzsch, K. C.; Rulkens, R.; Balaishis, D.; Ni, Y.; Pudelski, J. K.; Lough, A. J.; Manners, I.; Foucher, D. A. *Organometallics* **1996**, *15*, 1972.
(39) (a) Olympia, P. L., Jr.; Wei, I. Y.; Fung, B. M. *J. Chem. Phys.* **1969**, *51*, 1610. (b) Millar, J. M.; Thayer, A. M.; Zimmermann, H.; Pines, A. *J. Magn. Reson.* **1986**, *69*, 243.
(40) Mulay, L. N.; Attalla, A. *J. Am. Chem. Soc.* **1963**, *85*, 702.
(41) (a) Green, J. C. *Chem. Soc. Rev.* **1998**, *27*, 263. (b) Barlow, S. B.; Drewitt, M.; Dijkstra, T.; Green, J. C.; O'Hare, D.; Whittingham, C.; Wynn, H. H.; Gates, D. P.; Manners, I.; Nelson, J. M.; Pudelski, J. K. *Organometallics* **1998**, *17*, 2113.
(42) For a graphical representation of the proposed backbone motion of these polyferrocenylsilanes, please see: http://www.chem.utoronto.ca/staff/IM/animation1.gif and http://www.chem.utoronto.ca/staff/IM/animation1a.gif.
(43) Huang, T. H.; Skarjune, R. P.; Wittebort, R. J.; Griffin, R. G.; Oldfield, E. *J. Am. Chem. Soc.* **1980**, *102*, 7379.
(44) Simulations involving unrestricted rotation about the Si−O bond did not correlate with the observed line shapes for **2e**, and limited rotation about the Si−O bond seemed the most likely candidate for the increased mobility of the methoxy groups in comparison to **2d.**
(45) Wilkinson, G. *Org. Synth.* **1956**, *36*, 31.

MA021130Q